Quinolinate Phosphoribosyltransferase: Kinetic Mechanism for a Type II PRTase†

Hong Cao, Beth L. Pietrak,‡ and Charles Grubmeyer*

Fels Institute for Cancer Research and Molecular Biology and Department of Biochemistry, Temple University School of Medicine, 3307 North Broad Street, Philadelphia, Pennsylvania 19140

Received December 12, 2001

ABSTRACT: Quinolinate phosphoribosyltransferase (QAPRTase, EC 2.4.2.19) catalyzes the formation of nicotinate mononucleotide, carbon dioxide, and pyrophosphate from 5-phosphoribosyl 1-pyrophosphate (PRPP) and quinolinic acid (QA, pyridine 2,3-dicarboxylic acid). The enzyme is the only type II PRTase whose X-ray structure is known. Here we determined the kinetic mechanism of the enzyme from *Salmonella typhimurium*. Equilibrium binding studies show that PRPP and QA each form binary complexes with the enzyme, with K_D values (53 and 21 μM, respectively) similar to their K_M values (30 and 25 μM, respectively). Although neither PP_i nor NAMN products bound well to the enzyme, 130-fold tighter binding of PP_i ($K_D = 75$ μM) and NAMN ($K_D = 6$ μM) in a ternary complex was observed. Phthalic acid ($K_D = 21$ μM) and PRPP each caused a 2.5-fold tightening of the other's binding. Isotope trapping experiments indicated that the E·QA complex is catalytically competent, whereas the E·PRPP complex could not be trapped. Pre-steady-state kinetics gave a linear rate of NAMN formation, indicating that on-enzyme phosphoribosyl transfer chemistry is rate-determining. Isotope trapping from the steady state revealed that nearly all QA and about one-third of PRPP in ternary enzyme·QA·PRPP complexes could be trapped as the product. Substrate inhibition by PRPP was observed. These data demonstrate a predominantly ordered kinetic mechanism in which productive binding of quinolinic acid precedes that of PRPP. An E·PRPP complex exists as a nonproductive side branch.

The N-nucleosidic bond of purine, pyrimidine, and pyridine nucleotides is formed by the action of the phosphoribosyltransferases (PRTases,[1] nucleotide synthases). The last several years have seen remarkable growth in our knowledge of the structure and function of this enzyme group. A major finding is that the PRTases consist of two distinct evolutionary groups with distinct active site architecture (*1*). The first group, the type I PRTases, consists of HGPRTases (*2*), OPRTase (*3*), glutamine PRPP amidotransferase (GPAT; *4*), UPRTase (*5*), and PRPP synthase (*6*). Their architecture is of a Rossman fold, atop which loop and hood structures flank a solvent-exposed active site (*2*, *7*). In all cases studied to date, their kinetic mechanisms are sequential, with either functionally ordered (HGPRTase; *8*) or random (OPRTase; *9*) binding of substrates. The random component to the mechanism of type I PRTases is consistent with the observation from many X-ray structures of incomplete enzyme−substrate complexes that bound substrates have free access to solvent (*2*, *3*). The ordering of binding in HGPRTase is proposed to result from a PRPP-induced structural change. The second PRTase group, the type II enzymes, is represented by a single enzyme, QAPRTase, although NAPRTase may also be a type II PRTase (*10*). The X-ray structure of the dimeric *Salmonella typhimurium* QAPRTase has been determined as its enzyme·QA and enzyme·NAMN complexes at 3.0 Å resolution (*1*). In this case, the fundamental fold is an unusual seven-stranded α/β barrel containing the active site, with an α/β open sandwich structure that serves as a cap for the α/β barrel of the adjacent subunit. More recently, the hexameric *Mycobacterium tuberculosis* enzyme has been determined to 2.4 Å resolution as a catalytically unproductive enzyme·phthalate·PRPP complex (*11*). In this structure, it appears that the QA analogue phthalic acid lies at the bottom of a solvent-occluded active site, with bound PRPP positioned between it and the solvent, an arrangement quite distinct from that seen in the type I enzymes.

The QAPRTase reaction

$$QA + PRPP \rightarrow NAMN + PP_i + CO_2$$

provides the de novo source of NAMN for NAD biosynthesis (*12*, *13*). The enzyme is ubiquitous in distribution, and has been isolated from mammalian liver and brain, plants, and bacteria (*14*−*17*). The enzyme from *S. typhimurium* is a dimer of identical 32 428 Da subunits (*18*), and is stable in solution. Interest in the human central nervous system form of the enzyme has been fueled by the observation of high levels of the excitatory neurotoxin quinolinic acid in some degenerative brain diseases (*19*, *20*).

QAPRTase is unique among PRTases in catalyzing a decarboxylation linked to phosphoribosyl transfer. From both model studies (*21*) and enzyme experiments (*22*), the decarboxylation appears likely to occur via a hypothetical "quinolinate mononucleotide" intermediate, which is pro-

† Supported by NIH Grant GM48623.

* To whom correspondence should be addressed. Phone: (215) 707-4495. Fax: (215) 707-5529. E-mail: ctg@ariel.fels.temple.edu.

‡ Current address: Department of Biological Chemistry, Merck & Co., Sumneytown & West Point Pikes, West Point, PA 19486.

[1] Abbreviations: HGPRTase, hypoxanthine-guanine PRTase; KIE, kinetic isotope effect; NAMN, nicotinate mononucleotide; NAPRTase, nicotinate phosphoribosyltransferase; OPRTase, orotate PRTase; PRTase, phosphoribosyltransferase; QA, quinolinic acid; PP_i, pyrophosphate; UPRTase, uracil PRTase.

10.1021/bi012148g CCC: $22.00
Published on Web 02/14/2002

Scheme 1

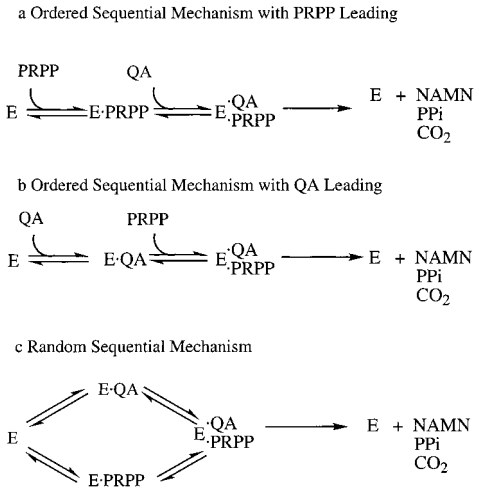

duced by phosphoribosyl transfer and may exist fleetingly on the enzyme surface or be released into solution. Ylide mechanisms have been proposed for the spontaneous decarboxylation of QAMN (*22*), but enzymic assistance has not been ruled out and could occur through a number of mechanisms. The decarboxylation step is chemically analogous to the reaction carried out by OMP decarboxylase, which is also an α/β barrel (*23*), and like QAPRTase uses no cofactor.

Because of its unusual chemistry, and its position as the sole documented representative of type II PRTases, the kinetic mechanism of QAPRTase is important. Calvo's group has completed two studies on the reaction. The first (*22*) used steady-state kinetics to deduce a sequential mechanism in which both PRPP and QA bind before PP_i, NAMN, or CO_2 is released. Three possible orders of substrate binding in the sequential kinetic mechanisms of QAPRTase may be proposed, as diagrammed in Scheme 1. Scheme 1a presents an ordered sequential mechanism with PRPP as the leading substrate. Scheme 1b shows an ordered sequential mechanism in which QA binding precedes that of PRPP. Scheme 1c presents a random sequential mechanism. Bhatia and Calvo (*24*) used patterns of product inhibition and dead-end inhibition by phthalic acid and fructose 1,6-bisphosphate to determine that QAPRTase followed mechanism 1a.

In the current work, equilibrium binding, isotope partitioning, and chemical quench experiments are used to document an ordered sequential mechanism with QA leading. An unproductive side branch in which PRPP binds first and binding of PRPP to E·phthalate complexes provide a rationale for earlier initial velocity and product inhibition kinetics data.

MATERIALS AND METHODS

Materials. [^{3}H]Quinolinic and [^{3}H]phthalic acids were purchased from Moravek Biochemicals, Inc. (Brea, CA). [γ-^{32}P]ATP was obtained from Amersham. [^{32}P]P_i and [^{32}P]-PP_i were purchased from Dupont NEN Research Products. Polyethyleneiminecellulose sheets for thin-layer chromatography (Macherey-Nagel Inc.) were obtained from Alltech (Deerfield, IL). Whatman 3MM chromatography paper, CF11 cellulose, all chromatography solvents, and other chemicals were from Fisher. [^{14}C]NA, NAMN, PRPP, and all other biochemicals were from Sigma. Econo-safe liquid scintillation cocktail was from Research Products International Corp. (Mt. Prospect, IL). *Escherichia coli* PRPP synthase was a kind gift of R. Switzer (*25*).

[β-^{32}P]PRPP and [5-^{32}P]PRPP (synthesized by B. Bizzle) were prepared enzymatically as described by Xu et al. (*8*) and Wang et al. (*26*), respectively. For synthesis of [^{14}C]-NAMN (performed by J. Gross), reaction mixtures contained 0.05 μg/mL NAPRTase, 1 mM [^{14}C]NA (54.8 mCi/mmol), 3 mM PRPP, 5 mM ATP, 15 mM $MgSO_4$, 5 mM DTT in 200 mM potassium glutamate, and 20 mM Tris-SO_4 (pH 8.3). After 30 min at 30 °C, 100 μL portions were injected onto a μBondapack C18 column equilibrated and eluted isocratically in 100 mM sodium acetate (pH 4.5). The [^{14}C]NAMN was then diluted 10-fold into 20 mM Tris-HCl (pH 7.5). Portions (1 mL) of the crude product were loaded onto a mono-Q column (0.5 cm $\times$ 6 cm) equilibrated in the same buffer and eluted with a 10 mL linear gradient to 0.5 M NaCl.

Enzyme Purification. Recombinant *S. typhimurium* QAPRTase was expressed and purified to homogeneity following the methods described by Eads et al. (*1*). The extinction coefficient of QAPRTase was determined by quantitative amino acid analysis of triplicate samples at the Protein Microchemistry Facility of the Wistar Institute (Philadelphia, PA). The resultant E_{280} of 0.82 for a 1 mg/mL solution was used throughout this work. The molarity of the homodimeric enzyme was calculated on the basis of an M_r of 64 856 (2 $\times$ 32 428; *18*).

Standard Assays. During enzyme purification, activity was determined using a colorimetric assay for the cyanide adduct of NAMN (*18*). For all other kinetic work, a continuous spectrophotometric assay based on the difference in extinction coefficients of QA and NAMN at 266 nm (ΔA_{266} = 920 M^{-1} cm^{-1}) was used. Assay mixtures typically contained 300 μM QA, 1 mM PRPP, and 6 mM $MgCl_2$ in 50 mM KH_2PO_4 buffer (pH 7.2), with 15−30 μg of QAPRTase. These mixtures were altered for determination of K_M values from initial velocity data. In experiments on PRPP substrate inhibition, spectrophotometric assay mixtures contained 50 mM KH_2PO_4, 6 mM $MgCl_2$, 25 μM QA, and 15−25 μg of QAPRTase. In this case, the MgPRPP concentrations were varied from 33 μM to 10 mM. Substrate inhibition kinetic parameters were evaluated with the HYPER program of Cleland (*27*), and other inhibition patterns were analyzed with COMP, NONCOMP, and UNCOMP.

Equilibrium Binding. The equilibrium gel filtration method of Hummel and Dreyer (*28*) modified by Grubmeyer et al. (*29*) was employed to assess ligand binding to the enzyme. All binding mixtures contained radiolabeled substrate with a second nonbinding compound containing a different radioactive isotope to serve as a volume indicator. The standard buffer consisted of 50 mM KH_2PO_4 and 6 mM $MgCl_2$ (pH 7.2). To quantify PRPP binding, mixtures also contained [β-^{32}P]PRPP and [^{3}H]glucose, with 100 μM phthalic acid present as noted. For QA binding, QAPRTase was equilibrated with [^{3}H]QA and [^{32}P]P_i in standard buffer, with 2 mM phthalic acid present as noted. Each enzyme ligand mixture was applied to a Sephadex G-50 column in a 1 mL tuberculin syringe preequilibrated and eluted with the same buffer containing the respective isotopes. The levels of radioactivity in the peak and the trough were averaged to calculate the extent of binding.

For binding of [^{3}H]phthalate, [^{32}P]PP_i, and [^{14}C]NAMN, a centrifugal dialysis method (modified from that from ref *30*) was employed. Equilibration mixtures (300 μL) containing enzyme and ligand in standard buffer were made. Nonradioactive PRPP (1 mM) was present in some experiments as noted in the text. A 50 μL sample was removed to determine the total amount of ligand by liquid scintillation. The remainder of the mixture was applied to a Microcon YM10 apparatus (Amicon). A centrifugation in a laboratory microcentrifuge at 8000 rpm for 2 min was employed to wash out liquid left in the apparatus by the manufacturer, which otherwise gave erroneous results. A second centrifugation at 14 000 rpm for 3 min was made into a fresh tube. A sample (50 μL) of this liquid was used to measure the amount of unbound ligand.

In all cases, data were analyzed using the format of Scatchard (*31*), fit by linear least squares.

Isotope Trapping. Isotope trapping experiments (*32*, *33*) were carried out at room temperature. For isotope trapping of [β-^{32}P]PRPP, 10 μL of an equilibrium enzyme ligand mixture containing 60 μM [β-^{32}P]PRPP and 60 μM QAPRTase in standard buffer was injected with a Hamilton syringe into a rapidly stirred 450 μL chase mixture containing 5 mM QA and 5 mM PRPP in standard buffer. For isotope trapping of QA, 10 μL of an equilibrium enzyme ligand mixture containing 30 μM [^{3}H]QA and 42 μM QAPRTase in standard buffer was injected into a rapidly stirred 450 μL chase solution containing 10 mM QA and 5 mM PRPP in standard buffer. In both reaction mixtures, after mixing had been carried out for 40 s ($\sim$20$-$30 turnovers), 100 μL of 0.5 M EDTA was added to the mixture to quench the reaction. As a control to ensure the efficiency of isotopic dilution, 10 μL of the apoenzyme was injected into 450 μL of a chase solution containing the respective isotope in each experiment. In all cases, a sample (10 μL) of the quenched [β-^{32}P]PRPP isotope trapping solution was applied to a polyethyleneiminecellulose plate and chromatographed with 0.85 M NaH_2PO_4 at pH 3.4. The [β-^{32}P]PRPP and [^{32}P]PP_i were visualized and quantified using a BAS2000 Fuji Bioimaging Analyzer. The quenched [^{3}H]QA trapping mixture was chromatographed on 3MM Whatman paper (20 cm $\times$ 20 cm) with a 4:6 mixture of 1 M ammonium acetate and 95% ethanol. The chromatographic origin was prespotted with nonradioactive QA or NAMN to allow visualization under 254 nm UV light. The spots were then cut out from the chromatogram, eluted in 0.1 mL of 0.1 N HCl, and subjected to liquid scintillation counting.

Rapid Mixing Experiments. Pre-steady-state kinetic experiments were performed using a model 1010 Precision Syringe Ram (Update Instrument Inc., Madison, WI) at room temperature. A two-syringe setup was employed, in which one syringe usually contained 400 μM [^{3}H]QA and 40 μM QAPRTase, while the other syringe contained 2 mM PRPP with 12 mM $MgCl_2$. KH_2PO_4 (50 mM, pH 7.2) was present in both syringes. Single-push (3$-$100 ms) and two-push ($>$100 ms) protocols were followed. After the reaction had been quenched in 450 μL of 0.9 N $HClO_4$, followed by centrifugation to remove the denatured protein, the pH of the supernatant was adjusted to pH 6$-$6.5 by adding 9 N KOH. Following centrifugation, a portion (100 μL) of the supernatant was chromatographed on a Waters μBondapak C18 column and eluted isocratically with 0.1% trifluoroacetic acid in H_2O. The separation of [^{3}H]QA and [^{3}H]NAMN was monitored at 230 nm, and the compounds were collected and quantified by liquid scintillation counting. To measure the degree to which the substrate [^{3}H]QA was contaminated by material chromatographing as [^{3}H]NAMN, 54 μL of a solution from the [^{3}H]QA syringe was thoroughly mixed with 450 μL of 0.9 N $HClO_4$, and 54 μL of solution from the enzyme syringe was added. These control samples were then treated like the experimental samples.

Steady-State Isotope Trapping. Steady-state isotope trapping (*34*) followed the same instrumental setup as described in the rapid mixing experiments, and made use of a two-push protocol. In duplicate reactions for each time point, the aged solution was ejected either into quench or into a rapidly stirred chase solution. After ejection into chase, samples were mixed for 40 s (10$-$20 turnovers) and the reactions quenched as described below.

For [^{3}H]QA steady-state isotope trapping, syringe A contained 40 μM QAPRTase and 400 μM [^{3}H]QA in 50 mM KH_2PO_4 (pH 7.2) and syringe B contained 2 mM PRPP and 12 mM $MgCl_2$ in 50 mM KH_2PO_4 (pH 7.2). The chase solution contained 10 mM QA, 1 mM PRPP, and 6 mM $MgCl_2$ in 50 mM KH_2PO_4 (pH 7.2). For "chase" samples, 40 μL of 9 N $HClO_4$ was added as a quench after the trapping process. For "quench" samples, the quench solution included all components of the chase solution and 40 μL of 9 N $HClO_4$. In both cases, the quenched reaction mixtures were processed by the same procedures as described for rapid mixing experiments.

For [5-^{32}P]PRPP steady-state isotope trapping, syringe A contained 2 mM QA, 40 μM QAPRTase, and 6 mM $MgCl_2$ in 50 mM KH_2PO_4 (pH 7.2). Syringe B contained 200 μM [5-^{32}P]PRPP, 6 mM $MgCl_2$, and 50 mM KH_2PO_4 (pH 7.2). The chase solution contained 1 mM QA, 3 mM PRPP, and 9 mM $MgCl_2$ in 50 mM KH_2PO_4 (pH 7.2). The chase period was 15 s. Formic acid (75 μL, 20 M) was employed as the quench. A 10 μL portion of each quenched reaction mixture was chromatographed on cellulose as described above. The [^{32}P]PRPP and [^{32}P]NAMN spots were visualized and quantified by phosphorimaging.

RESULTS

Substrate Binding. Equilibrium gel filtration experiments were performed to detect the binding of [β-^{32}P]PRPP and [^{3}H]QA to QAPRTase. PRPP bound to the *S. typhimurium* QAPRTase with a K_D of 53 $\pm$ 11 μM and an *n* of 2.1 mol of PRPP/mol of QAPRTase dimer (Figure 1; constants are summarized in Table 1). The K_D corresponds to K_M values of 30 and 16 μM for the *S. typhimurium* and *E. coli* forms of the enzyme, respectively (*18*, *24*). For QA binding (Figure 2), the Scatchard plot allowed the calculation of a K_D of 21 $\pm$ 7 μM with an *n* of 1.7 mol of QA/mol of QAPRTase dimer. The K_D is consistent with the K_M of 25 μM for the *S. typhimurium* and 6 μM for the *E. coli* QAPRTases. These results indicate that both substrates can bind to unliganded QAPRTase, but do not indicate whether the resultant binary complexes are catalytically competent. Although binding results are most consistent with the random mechanism of Scheme 1c, addition of nonproductive branches to mechanism 1a or 1b would allow them to accommodate these results.

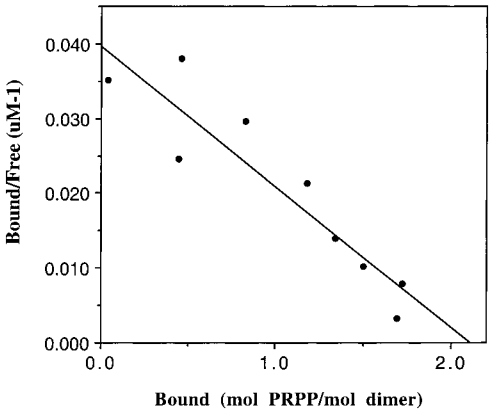

FIGURE 1: [β-^{32}P]PRPP binding to QAPRTase. The line was fit by linear least-squares regression. The value of K_D was 53 μM with an n of 2.1 mol of [β-^{32}P]PRPP/mol of QAPRTase dimer.

Table 1: Kinetic and Rate Constants Measured for QAPRTase

constant	value	constant	value
k_1[a]	1.5 μM^{-1} s^{-1}	$K_{i(PRPP)}$	2.2 mM
k_{-1}	24 s^{-1}	$K_{i(NAMN)}$	63 μM (vs QA)
k_2	0.04 μM^{-1} s^{-1}	$K_{D(NAMN)}$	800 μM
k_{-2}	0.8 s^{-1}	$K_{D(NAMN)}$ (with PP$_i$)	6.2 μM
k_{cat}	0.4 s^{-1}	$K_{D(PP_i)}$	>1.5 mM
$K_{D(QA)}$	22 μM	$K_{D(PP_i)}$ (with NAMN)	75 μM
$K_{M(QA)}$	25 μM[b]	$K_{i(phthalate)}$	44 μM (vs QA)
$K_{D(PRPP)}$	53 μM	$K_{D(phthalate)}$	21 μM
$K_{M(PRPP)}$	30 μM	$K_{D(phthalate)}$ (with PRPP)	8 μM

[a] See Scheme 2 for definitions. [b] From ref *18*.

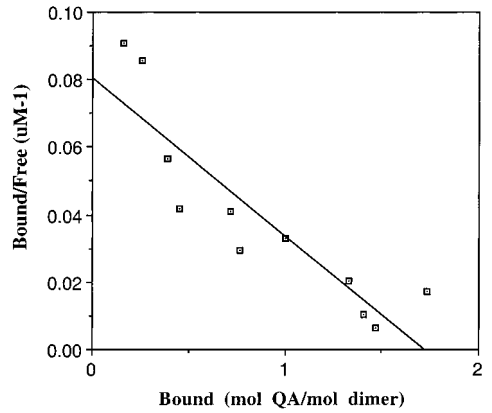

FIGURE 2: [^{3}H]QA binding to QAPRTase. The line was fit by linear least-squares regression. The K_D was 21 μM with an n of 1.7 mol of [^{3}H]QA/mol of QAPRTase dimer.

The binding of products NAMN and PP$_i$ was also examined by equilibrium gel filtration. No binding of [^{32}P]-PP$_i$ was detected. On the basis of the sensitivity of the assay, and the conditions that were employed, a minimal K_D of PP$_i$ is 1.5 mM. Bhatia and Calvo (*24*) reported K_i values of 0.5 and 2.2 mM for PP$_i$ inhibition of *E. coli* QAPRTase, consistent with our findings. Binding of [^{14}C]NAMN was weak. No Scatchard analysis was undertaken, but single-point determinations suggested a K_D of 800 $\pm$ 100 μM. In contrast, the reported K_i for NAMN was 27 μM (*24*). When the binding of [^{14}C]NAMN was examined in the presence of 1 mM PP$_i$, binding was observed, with a K_D of 6.2 $\pm$ 2.1 μM, and an n value of 1.1 mol of [^{14}C]NAMN/mol of dimer. This represents a tightening of NAMN binding of at least 130-fold induced by PP$_i$. A titration of the effect of PP$_i$ on [^{14}C]NAMN binding gave a half-maximal stimulation at 85 μM PP$_i$. Correction of this number for the 20 μM enzyme present suggests a K_D for PP$_i$ binding to the E·NAMN complex of 75 μM. If a thermodynamic box is drawn representing the random binding of PP$_i$ and NAMN to the apoenzyme in formation of the two binary complexes and one ternary complex, the binding of PP$_i$ to unliganded enzyme, required to be 130-fold looser than binding to the E·NAMN complex, must have a K_D of 15 mM, explaining why it was unobservable. The origin of the low n value for the binding of NAMN is not known.

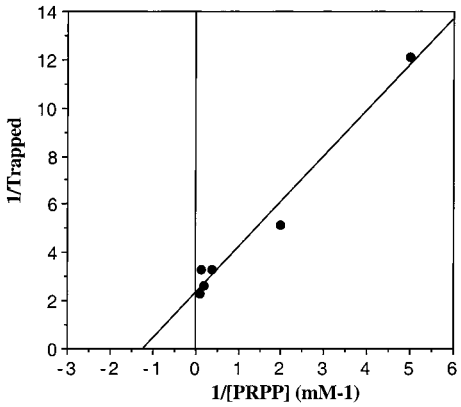

FIGURE 3: Double-reciprocal plot of the level of [^{3}H]QA trapping vs PRPP concentration. The line was fit by linear least-squares regression. The maximum amount of E·QA complex trapped was 70% of that bound, with half-maximum trapping achieved at 800 μM PRPP in the chase solution.

Isotope Trapping. Isotope trapping experiments (*32*, *33*) investigate the partitioning of binary and ternary enzyme−substrate complexes in the reaction pathway. For PRPP and QA substrates of the QAPRTase reaction, complexes of enzyme with radiolabeled substrate were formed, and then injected into a chase solution containing the second substrate, together with a large concentration of the nonradioactive form of the substrate whose behavior was to be analyzed. When QAPRTase·[β-^{32}P]PRPP complexes were injected into chase mixtures containing QA and nonradioactive PRPP, no [β-^{32}P]-PRPP was trapped as PP$_i$. Controls confirmed that the enzyme remained active during the incubation phase. The experiment was repeated under various conditions of active site occupancy by [β-^{32}P]PRPP to confirm the absence of trapping. These results are inconsistent with an ordered sequential mechanism with PRPP leading (Figure 1a) in which the E·[β-^{32}P]PRPP complex should be trapped, but are consistent with mechanism 1b, or the random mechanism 1c if PRPP is able to dissociate rapidly from the E·PRPP·QA Michaelis complex.

For [^{3}H]QA isotope trapping, 30 μM [^{3}H]QA and 42 μM QAPRTase subunit were present in the equilibrium binding solution prior to trapping. In this solution, 46% of the total ligand was bound to the enzyme, and 32% of the enzyme active sites were occupied by the ligand. Under these conditions, bound [^{3}H]QA was trapped as [^{3}H]NAMN when the complexes were injected into buffer containing PRPP and nonradioactive QA. The PRPP concentration in the chase solution was varied from 200 μM to 10 mM (Figure 3). The amount of E·[^{3}H]QA trapped exhibited a hyperbolic dependence on the PRPP concentration in the chase solution, with a maximum of 70% of the E·[^{3}H]QA complexes trapped. Half-maximal trapping was achieved at a PRPP concentration

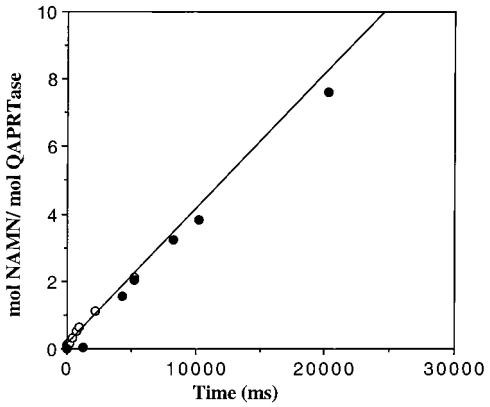

FIGURE 4: Rate of [^{3}H]NAMN formation. Rapid mixing experiments were performed as described in Materials and Methods. Black and white circles represent two separate experiments. The k_{cat} of the reaction was 0.4 s^{-1}.

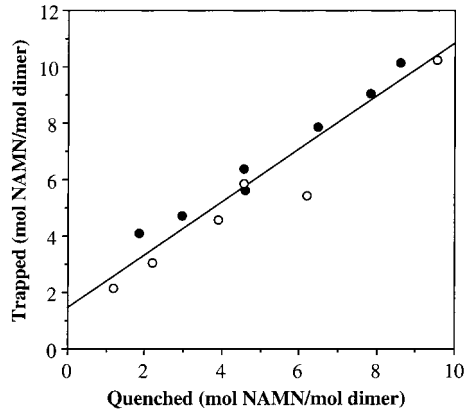

FIGURE 5: Steady-state isotope trapping of [^{3}H]QA. Steady-state isotope trapping experiments were performed as described in Materials and Methods. The extents of formation of [^{3}H]NAMN in reactions quenched at the steady state (Quenched) and reactions quenched after isotope trapping at the steady state (Trapped) were plotted against each other. Data from two experiments are shown as black and white circles. The line was fit by linear least-squares regression, generating a slope of 0.93 mol of NAMN trapped/mol quenched. The amount of [^{3}H]QA trapped from the steady state was 1.44 mol/mol of dimer.

of 800 μM. The trapping of enzyme-bound [^{3}H]QA indicates that mechanisms 1b and 1c are each possible, and is also inconsistent with mechanism 1a.

Phosphoribosyl Group Transfer. Rapid mixing experiments were performed on the *S. typhimurium* QAPRTase to document the rate of the on-enzyme phosphoribosyl group transfer in the presteady state (Figure 4). The time points in these experiments ranged from 2 ms to 20 s. A straight line fitting the time course could be extrapolated to the origin. The k_{cat} observed during the rapid mixing experiment was 0.40 s^{-1}, in agreement with the value reported previously in the standard assay (*18*). The lack of a burst of product formation in the forward reaction demonstrates that QAPRTase, a type II PRTase, displays slow phosphoribosyl transfer chemistry. This behavior is in contrast to the rapid phosphoribosyl transfer chemistry characteristic in the type I PRTases, including HGPRTase (*8*) and OPRTase (*26*). This result indicates that in the steady state at saturating substrate, QAPRTase must predominantly exist as E·PRPP·QA complexes, and that phosphoribosyl transfer chemistry is largely rate-limiting. Although the radioactive product formed from [^{3}H]QA behaved like [^{3}H]NAMN on chromatography, the experiment does not address whether a "QAMN" intermediate exists, only that its existence is fleeting under the current reaction and isolation protocols.

Steady-State Isotope Trapping. To differentiate between random and ordered sequential kinetic mechanisms (mechanisms b and c of Scheme 1), the partitioning of the E·QA·PRPP ternary complex was examined by steady-state isotope trapping experiments (*34*) with [^{3}H]QA and [5-^{32}P]PRPP. In these experiments, mixtures of enzyme and radioactive substrate allowed to reach the steady state were injected into a quench solution or into a trap solution containing a vast excess of the nonradioactive substrate. Trap samples were allowed to react for ~10 additional turnover times, and then the reactions were quenched. The amount of radioactive substrate bound in the steady state and committed to catalysis is indicated by the difference between trap and quench samples. The time points of the plots ranged from 2 to 20 s. The data from multiple experiments were plotted as the moles of product per mole of dimer of the reactions quenched from the steady state versus the moles of product per mole of dimer for corresponding trapped samples. The quenched versus trapped plot of the [^{3}H]QA steady-state isotope trapping (Figure 5) extrapolated to 1.44 mol of [^{3}H]NAMN/mol of QAPRTase dimer at time zero, indicating that 1.4 mol of the E·[^{3}H]QA·PRPP complex is bound in active sites and committed to catalysis during the steady state. A plot of quenched versus trapped [5-^{32}P]PRPP (Figure 6) extrapolated to 0.55 mol of [5-^{32}P]PRPP/mol of QAPRTase dimer at time zero. This indicates that during steady-state isotope trapping, ~0.55 mol of E·QA·[5-^{32}P]PRPP/mol of QAPRTase dimer is committed to catalysis. For each experiment, the slope of the line was close to 1.

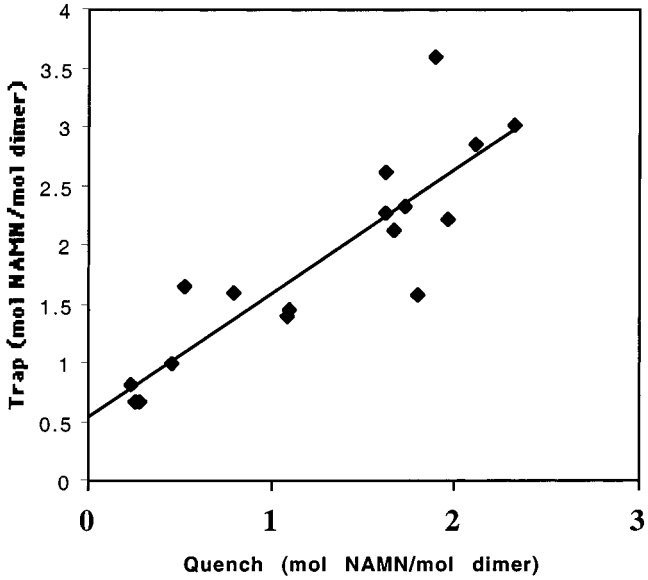

FIGURE 6: Steady-state isotope trapping with [5-^{32}P]PRPP. Experiments were performed as described in Materials and Methods. The extents of formation of [^{32}P]NAMN in reactions quenched from the steady state (Quench) and reactions quenched after isotope trapping from the steady state (Trap) were plotted against each other. Data from three experiments are shown. The line was fit by linear least-squares regression, generating a slope of 1.05 mol trapped/mol quenched The amount of [5-^{32}P]PRPP trapped from the steady state was 0.55 mol/mol of dimer.

Using the QA K_M of 20 μM, the PRPP K_M of 32 μM (*18*), and the experimental conditions, the amount of E·QA·PRPP

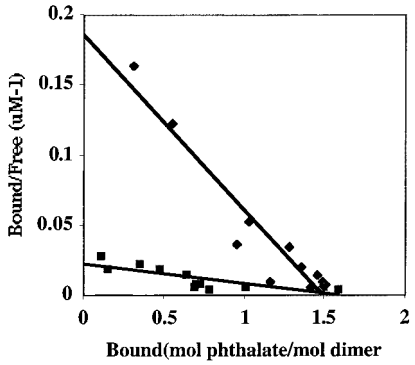

FIGURE 7: Binding of [^{3}H]phthalate to QAPRTase. [^{3}H]Phthalate binding was assessed by centrifugal dialysis as described in Materials and Methods, in the presence (◆) or absence (■) of 1 mM PRPP. The lines were fit by linear least-squares regression.

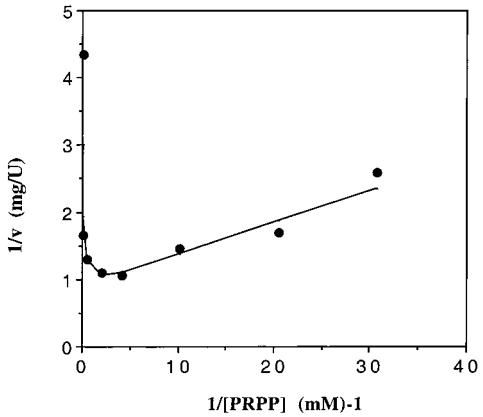

FIGURE 8: Substrate inhibition by PRPP. Assays were performed as described in Materials and Methods. The concentration of PRPP was varied from 33 μM to 10 mM, with the level of QA fixed at 25 μM. The data were fit with the HYPER program of Cleland (*8*), yielding a K_i of 2.2 ± 0.3 mM.

complex in the reaction system was estimated and compared with the amount of radioactive label trapped for each substrate. In the [5-^{32}P]PRPP steady-state isotope trapping, which contained 200 μM PRPP and 1 mM QA, 85 and 97% of the catalytic sites were occupied by PRPP and QA, respectively, giving a ternary complex occupancy of 82%. If two active sites per QAPRTase dimer are assumed, the observed trapping of the E·QA·[5-^{32}P]PRPP ternary complex was calculated to be 32% of the expected total amount of PRPP bound in ternary complexes. Using calculated occupancies of 87% for QA and 97% for PRPP, 85% of the active sites are in the form of ternary complexes in the [^{3}H]-QA steady-state isotope trapping experiments, for a [^{3}H]QA trapping efficiency of ~85%. The results clearly indicate that nearly all the [^{3}H]QA and about one-third of the [β-^{32}P]PRPP in E·QA·PRPP ternary complexes partition forward to product formation.

Interaction with Phthalic Acid. Phthalic acid (benzene-1,2-dicarboxylic acid) is a good inhibitor of QAPRTase with a reported K_i of 6 μM in the *E. coli* enzyme (*24*). Recently, the X-ray crystal structure of *Mycobacterium* QAPRTase cocrystallized with PRPP and phthalic acid was determined (*11*). In equilibrium gel filtration binding experiments with [^{3}H]QA, a phthalic acid concentration of 2 mM abolished [^{3}H]QA binding to QAPRTase (not shown), demonstrating that phthalic acid binds to the QA site. In the presence of 100 μM phthalic acid, QAPRTase has a K_D of 22 ± 3.4 μM for PRPP, binding approximately 2.4 times tighter to PRPP than in the absence of phthalic acid (not shown). Phthalic acid binding to QAPRTase had a K_D of 20.9 ± 4.7 μM, with an *n* value of 1.46 mol/mol of dimer (Figure 7). As demanded by the relevant thermodynamic box, in the presence of 1 mM PRPP, the K_D tightened 2.6-fold to 8.1 ± 1.9 μM with an *n* value of 1.5 mol of phthalate/mol of dimer.

Steady-State Kinetic Measurements. To resolve some of the differences between our conclusions and those of Bhatia and Calvo (*24*), selected steady-state kinetic measurements were undertaken using the direct spectrophotometric method. In agreement with published data, initial velocity experiments gave an intersecting pattern, with a $K_{M(QA)}$ of 14.0 ± 5.3 μM and a $K_{M(PRPP)}$ of 22.3 ± 9.9 μM. The product NAMN was competitive versus QA, with a K_i of 63.0 ± 28.8 μM (no pattern for this inhibitor vs QA was reported previously). Phthalate was found to be a competitive inhibitor versus QA, with a K_i of 44.1 ± 12.6 μM, higher than the value of 6 μM previously reported for the *E. coli* enzyme. When the QA concentration was fixed at 200 μM, inhibition by phthalic acid over 25−500 μM PRPP gave a pattern of parallel lines (Figure 7) that was well fit by uncompetitive inhibition (K_i = 128 ± 11 μM), as noted (*24*).

Since QAPRTase can bind PRPP (Figure 1), and the E·PRPP complex is catalytically nonproductive, high PRPP concentrations should cause substrate inhibition. We investigated this possibility using steady-state kinetics. The QA concentration was kept constant at a K_M level of 25 μM (*35*), and the PRPP concentrations were varied from 33 μM to 10 mM (Figure 8). Under these conditions, inhibition by PRPP was observed with a K_i of 2.2 mM.

Kinetic isotope effects (KIEs) provide an alternative route for assessing the partitioning of intermediates in enzymatic reactions. The KIE for [1-^{3}H]PRPP was measured to be 1.10 ± 0.02. The observed KIE in competitive experiments is a function of the intrinsic KIE (^3k) for the isotopically sensitive step, a ratio of summed "commitment factors" (c_f and c_r) expressing how the intermediate partitions toward dissociation of products or substrates, and the equilibrium isotope effect ($^3K_{eq}$) (*36*).

$$\mathrm{KIE} = ({}^3k + c_f + c_r {}^3K_{eq})/(1 + c_r + c_f)$$

The overall QAPRTase reaction is irreversible, allowing the reverse commitment factor to be set at 0, permitting simplification to

$$\mathrm{KIE} = ({}^3k + c_f)/(1 + c_f)$$

The steady-state isotope trapping allowed the independent determination of c_f for PRPP (0.47). Thus, ^3k = 1.147. For ADP ribosylation reactions in which the C1−N1 bond of NAD is broken, 1-^{3}H intrinsic isotope effect values of ~1.20 have been measured (*37*), indicative of oxocarbenium-like transition states. For the NAMN-producing NAPRTase operating in the absence of ATP, a value of 1.14 was measured (C. Grubmeyer, unpublished observations). The uncoupled NAPRTase reaction is known to proceed without forward or reverse commitments (J. Gross and C. Grubmeyer, unpublished observations), suggesting the observed KIE is close to the intrinsic value. The existence of a nonunitary

Scheme 2

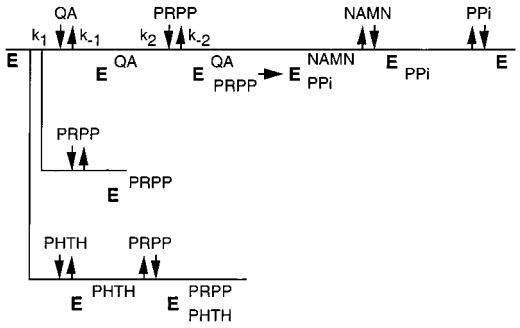

value for QAPRTase KIE confirms the finding from steady-state isotope trapping that [1-^{3}H]PRPP bound in ternary complexes is not irreversibly committed to catalysis.

DISCUSSION

The central conclusion from the current work is that *S. typhimurium* QAPRTase primarily follows an ordered substrate binding mechanism in which binding of QA precedes that of PRPP (Scheme 2). This mechanism is compatible with the known structure of QAPRTase−ligand complexes (*11*), but is in part inconsistent with the PRPP-leading ordered sequential mechanism previously determined (*24*). The major discrepancies result from the existence of nonproductive branches on the reaction pathway, with an unproductive E·PRPP complex, the ability of PRPP to bind to and stabilize complexes inhibited by E·phthalate complexes, and a tight dead-end E·NAMN·PP_i product complex.

The current evidence for an ordered mechanism comes from the behavior of preformed E·QA and E·PRPP complexes in isotope partitioning experiments. Although PRPP binding to a single class of two sites on the dimeric enzyme was documented here, E·PRPP complexes failed to partition toward the PP_i product in trapping experiments. If the mechanism were in fact random, the failure of QA to trap preformed E·PRPP complexes might be attributable to fast PRPP dissociation from an active ternary E·QA·PRPP complex. However, the ability to trap one-third of the E·QA·PRPP from the steady state shows that the ternary complex must be quite stable on the catalytic time scale. Thus, an ordered mechanism in which PRPP binds first is ruled out.

The behavior of PRPP was in marked contrast to that of QA, which also bound to unliganded enzyme, and which gave good trapping from either E·QA complexes or from E·QA·PRPP ternary complexes in the steady state. Together, this behavior is consistent with an ordered mechanism with QA leading. A strictly ordered mechanism with QA leading should allow for isotope trapping of 100% of the bound QA at an infinite PRPP concentration, but experimentally, only 70% was trapped, indicating the possibility of a random component for substrate dissociation. A random mechanism of substrate association is both unlikely and physiologically insignificant, based on the inability to trap bound PRPP with 5 mM QA. However, it is not possible to rule out the possibility that even higher concentrations of QA would allow capture of an E·PRPP complex.

Our binding results also have bearing on the order of product dissociation. Since NAMN is a potent inhibitor (see below), but only binds well to E·PP_i complexes (K_D = 6 vs 800 μM for binding to the apoenzyme), NAMN must be released first from E·NAMN·PP_i complexes, and be able to rebind to resulting E·PP_i complexes. In contrast, although it can bind to E·NAMN with a K_D of ~75 μM, pyrophosphate is a weak inhibitor, suggesting that it is released after NAMN. A random mechanism of product release, with slower release of PP_i, could also be accommodated by the binding data.

Bhatia and Calvo showed that F16BP and phthalic acid were inhibitors of QAPRTase, and used their inhibition patterns to deduce mechanism 1a (*24*). F16BP, a potential analogue of PRPP, was a weak competitive inhibitor versus that substrate (K_i = 3.5 mM), and noncompetitive versus QA (K_i = 10.9 mM). These patterns are in accord with an ordered mechanism in which PRPP (and its dead-end analogue F16BP) binds only to the unliganded enzyme. A purely ordered mechanism with QA binding first should yield uncompetitive inhibition by a PRPP analogue versus QA. However, it is likely that the demonstrated ability of PRPP to bind to either the apoenzyme or the E·QA complex is shared by F16BP. In inhibition experiments, increasing QA concentrations would compete with F16BP for binding to E, but would not affect F16BP binding to the E·QA complex, so that F16BP would produce both intercept and slope effects (noncompetitive inhibition) versus QA.

As expected from its resemblance to QA and in agreement with the current binding studies, phthalate produced competitive inhibition versus QA. At moderate (10K_M) levels of QA, phthalate inhibition appeared to be uncompetitive versus PRPP (K_i = 128 μM). Bhatia and Calvo also observed uncompetitive (K_i = 21 μM) inhibition by phthalate versus PRPP, the behavior expected from mechanism 1a, instead of the noncompetitive pattern expected from mechanism 1b. For either mechanism 1a or 1b, the intercept effect of phthalate is expected. However, if the unliganded enzyme and the E·phthalate complex can each bind PRPP, then high levels of PRPP will have two contrary effects: binding productively to E·QA complexes and trapping unproductive E·PRPP and E·phthalate·PRPP dead-end complexes. The trapping effect of the second substrate on a nonproductive analogue of the first substrate is well-known (*35*), and was proposed to lead to infinitesimal K_i values at an infinite concentration of the second substrate. These two effects may offset to give a pattern of uncompetitive inhibition versus PRPP.

Using the data gathered here, rough estimates can be made of several of the rate and equilibrium constants for the mechanism (Scheme 2 and Table 1). The response of QA trapping to PRPP concentration allowed us to determine half-maximal trapping at 800 μM PRPP. Thus, at this concentration, the rate of QA dissociation from E·QA complexes (k_{-1}) is equal to the rate of PRPP binding (k_2) times the PRPP concentration. Using the k_{cat}/K_M for PRPP (0.013 μM^{-1} s^{-1}) and the finding that one-third of the bound PRPP in E·QA·PRPP complexes partitions forward in the steady state, k_2 = 3(0.013 μM^{-1} s^{-1}) = 0.04 μM^{-1} s^{-1}. The rate of PRPP binding at 800 μM is calculated to be 32 s^{-1}. Using this value (32 s^{-1}) as k_{-1} and the measured value of K_1 permits the calculation of the QA on-rate (k_1, 1.5 μM^{-1} s^{-1}). By comparison, k_{cat}/K_M for QA gives a value of 0.016 μM^{-1} s^{-1}, 100-fold lower. This discrepancy comes about from PRPP inhibiting QA binding, and is explored below. An estimation of k_{-2}, the off-rate for dissociation of PRPP from

ternary complexes, can be made by calculation from the partition coefficient of enzyme-bound PRPP from the steady state [$P_c = k_{cat}/(k_{cat} + k_{-2})$]. Using the finding that one-third of the bound PRPP is trapped from the steady state (P_c = 0.33), $k_{-2} = 0.8\ s^{-1}$, giving a K_2 of 0.05×10^6 M ($1/K_2$ = 20 μM). The approximate 2.5-fold tightening of PRPP binding in ternary E·PRPP·QA complexes is in agreement with the 2.6-fold effect seen with phthalate-induced tightening of PRPP binding.

Since PRPP binds unproductively to unliganded QAPRTase, it should cause substrate inhibition, as E·PRPP complexes deplete the concentration of free QAPRTase. Substrate inhibition by PRPP was in fact noted (Figure 8). Surprisingly, the K_i, 2.2 mM, was far above the measured K_D for PRPP of 0.05 mM. However, inhibition in the steady state is dynamic, and is dominated by rate constants rather than equilibrium constants. The rate constant for equilibration of E and 25 μM QA is the sum of the on-rate and off-rate for that substrate ($k_{eq} = k_1[QA] + k_{-1}$), and is determined to be 62 s^{-1}. To reach a comparable rate for equilibration of E and PRPP (using $k_{eq} = k_2[PRPP] + k_{-2}$) requires ~1500 μM PRPP, close to the measured value for substrate inhibition. In fact, the situation is more complex in that E·QA complexes are removed by the productive binding of PRPP, and because binding of PRPP to E is 2.5-fold less tight than binding to the E·QA complex. The latter is difficult to include in any model because it is not known whether it is PRPP on-rates or off-rates, or both, that are changed when QA is bound. Despite this limitation, it was possible to model substrate inhibition using KinSim (*38*), using the branched kinetic pathway of Scheme 2 and rate constants determined above, and maintaining the same rates for PRPP binding to the unliganded enzyme as for E·QA complexes. Simulation results (not shown) were in good accord with the experimental data in predicting a macroscopic K_M for QA of 33 μM, and that 4 mM PRPP would cause 50% inhibition at 20 μM quinolinate. The slightly more potent substrate inhibition by PRPP observed experimentally may arise from the predicted 2.5-fold looser binding of PRPP to the unliganded enzyme.

The ability of PRPP to bind unproductively to E predicts an additional interesting kinetic anomaly. Under typical conditions for measurement of the K_M for QA (1 mM PRPP and 20 μM QA), ~97% of the enzyme is present as E·PRPP and E·QA·PRPP complexes, and only ~1% is in the free form. If simulations are run in which PRPP is not allowed to bind to the unliganded enzyme, the simulation K_M for QA drops to ~1 μM, in accord with the deviation between k_1 and the measured k_{cat}/K_M for QA noted above.

The QAPRTase reaction (rate of 0.4 s^{-1}) is slow compared to those of other PRTases in the type I group, which proceed at rates of 20−100 s^{-1}, and whose internal chemistry steps range from 100 to 300 s^{-1} (*26*). NAPRTase, in its phosphorylated form, catalyzes group transfer at 500 s^{-1}, in a sequence with an overall k_{cat} of 2.5 s^{-1}. The nonphosphorylated enzyme proceeds at a rate of 0.3 s^{-1}, with a rate-limiting chemical step. QAPRTase has been proposed to be phosphorylated (*18*), but the catalytic significance of the phosphorylation remains unkown.

The predominantly ordered mechanism for QAPRTase can also be compared with those of other enzymes in the PRTase group. In QAPRTase, an ordered mechanism with base leading is enforced by the structure of the enzyme's active site, which appears to block access for QA when PRPP is bound. In NAPRTase, for which no structure is known, but which has been proposed to be a member of the type 2 group by weak sequence similarity (*10*), the order of the forward reaction catalyzed by the phosphorylated enzyme is PRPP leading. For OPRTase, a type 1 PRTase, the order of both substrate binding and product release is clearly random (*26*), a finding in good agreement with the solvent-exposed active site. In HGPRTases, also type 1, trapping experiments show that productive substrate binding is ordered, with PRPP leading in the forward direction and nucleotide in the reverse (*8*). However, this order is not directly enforced by the structure of the unliganded active site, which appears to be open to both substrates, but is probably the result of a PRPP-induced enzyme isomerization which tightens base binding (*39*). Since products can be released in random fashion in either direction, and a tight E·PP_i·hypoxanthine complex has been documented, HGPRTase is only functionally ordered, a conclusion which may be important in drug design.

REFERENCES

1. Eads, C. J., Ozturk, D., Wexler, T. B., Grubmeyer, C., and Sacchettini, J. C. (1996) *Structure 5*, 47−58.
2. Eads, J. C., Scapin, G., Xu, Y., Grubmeyer, C., and Sacchettini, J. C. (1994) *Cell 78*, 325−334.
3. Scapin, G., Grubmeyer, C., and Sacchettini, J. C. (1994) *Biochemistry 33*, 1287−1294.
4. Smith, J. L. (1998) *Curr. Opin. Struct. Biol. 8*, 686−694.
5. Schumacher, M. A., Carter, D., Scott, D. M., Roos, D. S., Ullman, B., and Brennan, R. G. (1998) *EMBO J. 17*, 3219−3232.
6. Eriksen, T. A., Kadziola, A., Bentsen, A. K., Harlow, K. W., and Larsen, S. (2000) *Nat. Struct. Biol. 7*, 303−308.
7. Smith, J. L. (1999) *Nat. Struct. Biol. 6*, 706.
8. Xu, Y., Eads, J., Sacchettini, J. C., and Grubmeyer, C. (1997) *Biochemistry 36*, 3917−3924.
9. Bhatia, M. B., Vinitsky, A., and Grubmeyer, C. (1990) *Biochemistry 29*, 10480−10487.
10. Rajavel, M., Lalo, D., Gross, J. W., and Grubmeyer, C. (1998) *Biochemistry 37*, 4181−4188.
11. Sharma, V., Grubmeyer, C., and Sacchettini, J. C. (1998) *Structure 6*, 1587−1599.
12. Tritz, G. J. (1987) in *Escherichia coli and Salmonella typhimurium: Cellular and Molecular Biology* (Neidhardt, F. C., Ed.) pp 557−563, American Society for Microbiology Press, Washington, DC.
13. Penfound, T., and Foster, J. F. (1996) in *Escherichia coli and Salmonella typhimurium: Cellular and Molecular Biology* (Neidhardt, F. C., Ed.) 2nd ed., pp 721−730, American Society for Microbiology Press, Washington, DC.
14. Okuno, E., and Schwarcz, R. (1985) *Biochim. Biophys. Acta 841*, 112−119.
15. Okuno, E., White, R. J., and Schwarcz, R. (1988) *J. Biochem. 103*, 1054−1059.
16. Packman, P., and Jakoby, W. (1965) *J. Biol. Chem. 240*, 4107−4108.
17. Mann, D. F., and Byerrum, R. (1974) *J. Biol. Chem. 249*, 6817−6823.
18. Hughes, K. T., Dessen, A., Gray, J. P., and Grubmeyer, C. (1993) *J. Bacteriol. 175*, 479−486.
19. Reinhard, J. F., Jr., Erickson, J. B., and Flanagan, E. M. (1994) *Adv. Pharmacol. 30*, 85−127.
20. Heyes, M. P., Saito, K., Lackner, A., Wiley, C. A., Achim, C. L., and Markey, S. P. (1998) *FASEB J. 12*, 881−896.
21. Dunn, G. E., and Thimm, H. F. (1977) *Can. J. Chem. 55*, 1342−1347.
22. Kalikin, L., and Calvo, K. C. (1988) *Biochem. Biophys. Res. Commun. 152*, 559−564.

23. Harris, P., Navarro Poulsen, J. C., Jensen, K. F., and Larsen, S. (2000) *Biochemistry 39*, 4217−4224.
24. Bhatia, R., and Calvo, K. C. (1996) *Arch. Biochem. Biophys. 325*, 270−278.
25. Hove-Jensen, B., Harlow, K. W., King, C. J., and Switzer, R. L. (1986) *J. Biol. Chem. 261*, 6765−6771.
26. Wang, G., Lundegaard, C., Jensen, K. F., and Grubmeyer, C. (1999) *Biochemistry 38*, 275−283.
27. Cleland, W. W. (1979) *Methods Enzymol. 63*, 103−138.
28. Hummel, J. P., and Dreyer, W. J. (1962) *Biochim. Biophys. Acta 63*, 530−532.
29. Grubmeyer, T. C., Chu, K.-W., and Insinga, S. (1987) *Biochemistry 26*, 3369−3373.
30. Stitt, B. L. (1988) *J. Biol. Chem. 263*, 11130−11137.
31. Scatchard, G. (1949) *Ann. N.Y. Acad. Sci. 51*, 660−672.
32. Rose, I. A. (1980) *Methods Enzymol. 64*, 47−59.
33. Rose, I. A. (1995) *Methods Enzymol. 249*, 315−340.
34. Wilkinson, K. D., and Rose, I. A. (1979) *J. Biol. Chem. 254*, 12567−12572.
35. Segel, I. H. (1975) *Enzyme Kinetics*, John Wiley, New York.
36. Northrop, D. B. (1982) *Methods Enzymol. 87*, 607−624.
37. Scheuring, J., and Schramm, V. L. (1997) *Biochemistry 36*, 8215−8223.
38. Barshop, B. A., Wrenn, R. F., and Frieden, C. (1983) *Anal. Biochem. 130*, 134−145.
39. Heroux, A., White, E. L., Ross, L. J., Davis, R. L., and Borhani, D. W. (1999) *Biochemistry 38*, 14495−14506.

BI012148G